CONTACT DAMAGE RESPONSE OF CARBON FIBRE SKIN/CLOSED-CELL ALUMINIUM FOAM SANDWICH COMPOSITES

Maizlinda I. Idris[a,b], Tania Vodenitcharova[a] and Mark Hoffman[a]
[a]School of Materials Science and Engineering, University of New South Wales Sydney, NSW 2052, Australia; ARC Centre for Excellence for Design of Light Metals
[b]Faculty of Mechanical and Manufacturing Engineering, University of Tun Hussein Onn Malaysia, 86400 Parit Raja Batu Pahat Johor, Malaysia

Keywords: *Composite Skin; Metal Foam; Indentation; Remnant Strength*

Abstract

The contact damage response of sandwich composites made of closed-cell aluminium foam core (ALPORAS) and carbon fibre skin has been experimentally investigated. Quasi-static indentation tests on a series of core thicknesses were undertaken with indenters of different diameters. The behaviour of the damaged samples was then studied in four-point bending. It was shown that the contact damage on the surface of the sandwich samples is dependent only on the indenter diameter but independent of the sample thickness. The remnant compressive/tensile strength was also assessed. The results revealed that the undamaged samples exhibit higher strength than the damaged samples.

1 Introduction

Previously, many researchers focused their work on the fabrication of sandwich panels made of metallic core and metallic skin [4, 5, 8], metallic honeycomb core and fibre-reinforced polymers (FRP) skin [6], and polymer foam core and FRP skin [7, 9]. There is limited research on sandwich composites comprising aluminium foams and FRP skin, especially on their contact damage behaviour. Such a study is reported by Vaidya et *al* [1] which investigated the impact and vibrational behaviour of those panels and found out that S2-glass/VE facesheet provides a higher absorbed impact energy than the E-glass, aramid or carbon fiber reinforced vinyl ester (VE) resin skins. It is the aim of the present paper to study the behaviour of locally damaged panels in four-point bending, and assess their remnant compressive/tensile strength.

Aluminium foam was chosen as a core material because of its suitability for structural applications and high impact energy absorption. FRP skin possesses high specific strength and stiffness, and good corrosion resistance. Hence, a sandwich structure made of FRP skins separated by a low density aluminium foam core may superpose the advantages of both materials– for example, increased flexural stiffness (EI) without a significant weight increase [1, 2].

Sandwich structures often demonstrate a dramatic reduction in mechanical integrity following impact from damage, such as tool drop, hailstones, bird strikes and runway debris. This damage has been demonstrated to significantly reduce the structural properties of the skin, the interface and the core, or all the components of the sandwich system. The present paper investigates the response of sandwich panels made of closed-cell aluminium foam core and a carbon fiber reinforced epoxy skin, to indentation, and studies the effect of the induced damage on the remnant strength in bending of those panels.

2 Material and Experimental Procedure

2.1 Material

Sandwich composite panels of laminate 2/2 twill carbon fibre skin (MTM56/CF0300 – Advanced Composites Group Material, UK) and closed-cell aluminium foam panels (ALPORAS – Gleich Gmbh) were fabricated by hot-pressing. The sandwich samples were assembled on a hot press

machine at 100°C and a pressure of 0.1 MPa, and then cured for 120 minutes. An epoxy adhesive film (MTA240/PK13-313 – Advanced Composites Group, UK) was placed at the interface between the skin and the foam core, to ensure good bonding. The sandwich composite samples were fabricated with foam thicknesses of 8, 10 and 15 mm. The foam cell size was approximately 2.5mm and the relative density was around ~ 8%.

2.2 Quasi-Static Indentation Test

Quasi-static indentation tests were performed using an INSTRON 1185 universal testing machine with a 10 kN load cell.

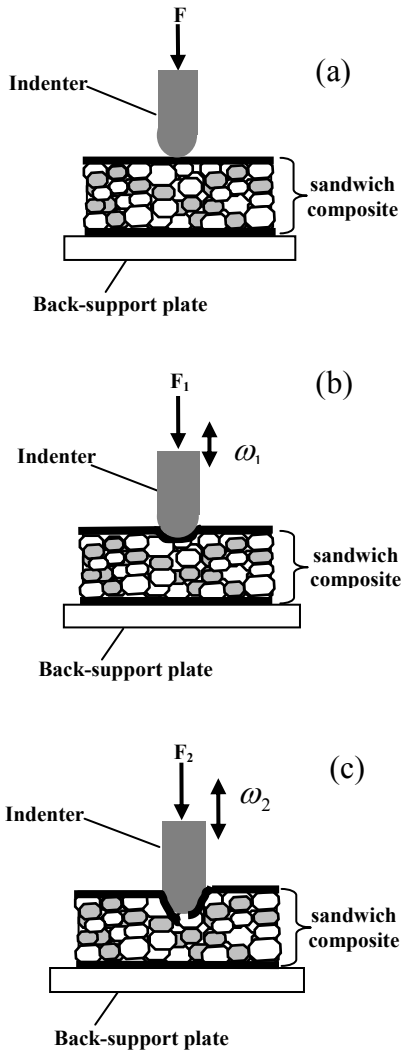

Fig.1. Schematic diagrams of a contact damage experiment: (a) prior to loading; (b) initial stage of indentation and onset of yielding of both skin and foam; (c) deep indentation causing continuing yielding of the foam and breakage of the skin. F is the indentation load, and ω is the indentation depth.

Spherical indenters of 5, 10 and 15 mm diameter were used to generate the contact damage. Indentation was undertaken at a constant cross-head displacement rate of 0.50 mm/min. Fig. 1 shows a schematic diagram of the contact damage experiment. The formation of the contact damage in the sample is influenced by the indentation depth. This experiment first identifies the minimum indentation depth at which contact damage in the core is induced without breaking the skin. The effect of the indenter diameter and the sample thickness is also investigated, and the corresponding load-indentation depth curves are recorded.

2.3 Four-Point Bending Test

The remnant strength in bending of both undamaged and damaged samples was assessed through four-point bending tests which were carried out according to ASTM 393-00. The sample dimensions were 280 mm × 40 mm, and the thickness was varied. The contact damaged region was located between the middle rollers (Fig.2 (a)). The distance between the loading rollers L_1,was chosen to be 50 mm, and the span length L_2 was fixed at 250 mm. Tabs were placed under the rollers to ensure that the load is distributed more evenly (Fig.2 (b)). The remnant strength of the samples was measured with the damaged region on both the compressive and tensile faces, (Fig.3).

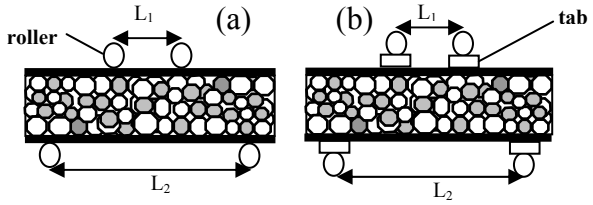

Fig.2. Schematic diagrams of a four-point bending test: (a) without tabs under the loading rollers; (b) with tabs.

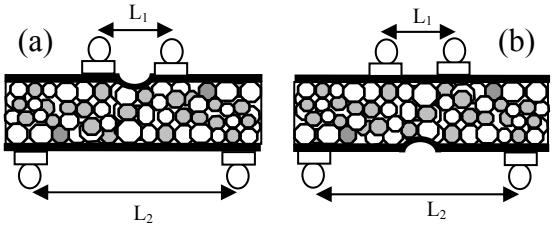

Fig.3. Schematic diagrams of remnant strength measurements: (a) the local damage is located in the compressive zone; (b) the local damage is located in the tensile zone.

The maximum stress at failure on both the compressive and the tensile skin and core surfaces was found for samples which had been damaged on one surface only. Undamaged samples were also tested for reference. The bending strength was calculated according to the following [3]:

$$(\sigma_f)_{\max} = \frac{MhE_f}{2D} \quad (1)$$

$$(\sigma_c)_{\max} = \frac{McE_c}{2D} \quad (2)$$

where D is the flexural stiffness, i.e.,

$$D = E_f \frac{bt^3}{6} + E_f \frac{btd^2}{2} + E_c \frac{bc^3}{12} \approx E_f \frac{btd^2}{2} \quad (3)$$

$(\sigma_f)_{\max}$ is the maximum skin stress at failure, $(\sigma_c)_{\max}$ is the maximum core stress at failure, M is the bending moment, E_f is the skin Young's modulus, E_c is the core Young's modulus, b is the sample width, t is the skin thickness, c is the core thickness, h is sample thickness and d is the distance between the centroidal axes of both skins.

3 Results and Discussions

3.1 Contact Damage on Sandwich Panels

Quasi-static indentation tests were carried out on one surface of the sandwich panels and at different indentation depths. The objective was to find the minimum indentation depth $\omega_{\min}$ at which no contact damage was generated in the core and no breakage was induced in the skin, for all indenter diameters and panel thicknesses.

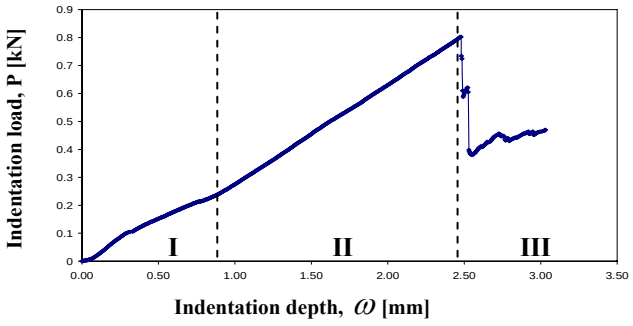

Fig.4. Load-displacement curve in indentation

A typical load-indentation curve in quasi-static indentation is shown in Fig. 4. Three main regions can be distinguished: Region I exhibits the early stage of the indentation process when the aluminium foam starts to yield; Region II corresponds to deeper indentation depths when both the skin and the foam yield; and Region III relates to a skin failure, and a penetration of the indenter into the foam through the broken skin. From the indentation tests, it was concluded that the contact damage is dependent on the indenter diameter but independent of the sample thickness. The minimum indentation depths for each indenter diameter are listed in Table 1, which shows that the $\omega_{\min}$ increases with the indenter diameter increasing. $\omega_{\min}$ is identified as the deflection at which the load is maximum. For example, Fig.5 shows the load-displacement curve in indenting sandwich panels of thicknesses of h = 8, 10 and 15 mm, using a 15 mm spherical indenter. $\omega_{\min}$ was found to be 3 mm for all the sample thicknesses.

Table 1. Minimum indentation depth for each indenter diameter

Indenter diameter, Ø (mm)	Indentation depth for skin failure, $\omega_{\min}$ (mm)
5.00	1.50
10.00	2.50
15.00	3.00

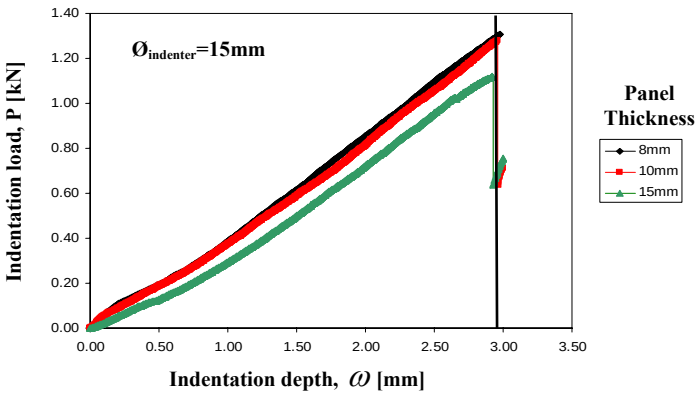

Fig.5. Minimum depths in indentation with a 15 mm spherical indenter

Macrostructural observations clearly show that the foam yields but the skin only deforms without breakage (Fig.6. (a) and (b)). This condition relates to Region II in Fig. 4. With the increase in the indentation depth, however, the skin fails, the indenter penetrates into the sample, Fig.6.(c)–(d),

and the mechanical properties of the sample are affected (Region III).

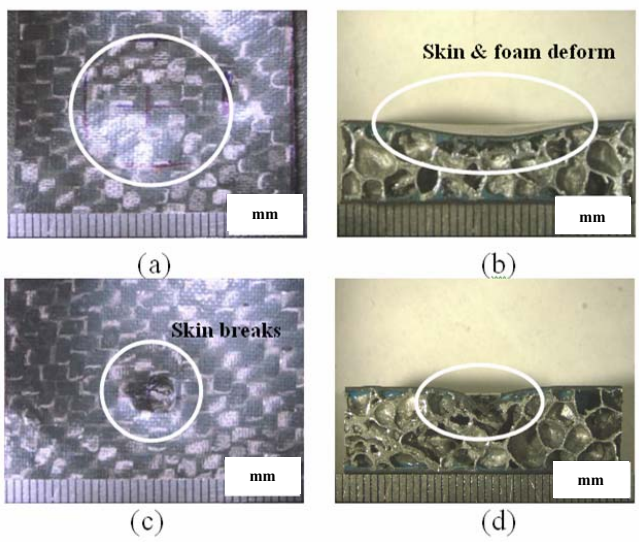

Fig.6. Macrostructures of indented samples: (a) surface and (b) subsurface of an undamaged skin with a deformed foam; (c) surface and (d) subsurface of a sample with a broken skin.

3.2 Energy absorption

3.2.1 Energy absorption in indentation

The absorbed energy in indentation W_i was also calculated as the area under the load-indentation curve. The values were normalized by the thickness h of the panels. It is clear from Fig. 7 that for the same h, W_i increases proportionally with the indenter diameter increasing; thus, the energy is higher for larger indenters. The energy though decreases when the sample thickness increases, thus thicker samples absorb less energy and the thinner samples have higher normalised energy absorption capacity.

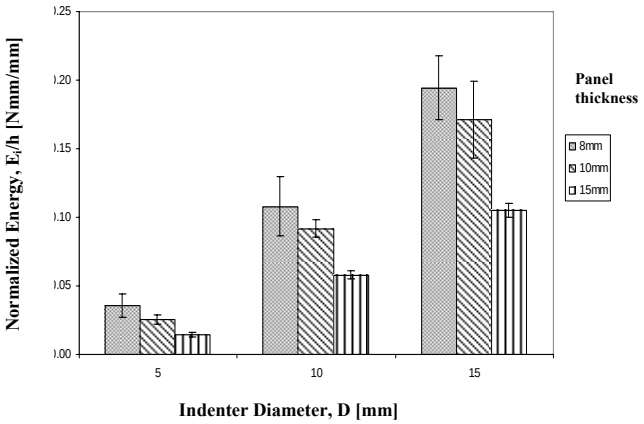

Fig.7. Energy absorption in quasi-static indentation, W_i normalized by the panel thickness h

3.2.2 Energy absorption in bending

Apart from the absorbed energy in indentation W_i, the absorbed energy in bending W_b was also analysed to determine its dependence on the area of the contact damage, panel thickness and location of the contact damage in both compressive and tensile condition. Figure 8 reveals that the absorbed energy in compression condition W_{bc} decreases if the contact damage enlarges since the damage weakens the panel. If W_{bc} is normalized by the panel thickness h, it is obvious that as h increases, the absorbed energy per unit panel thickness decreases, for the same contact damage (Fig. 9).

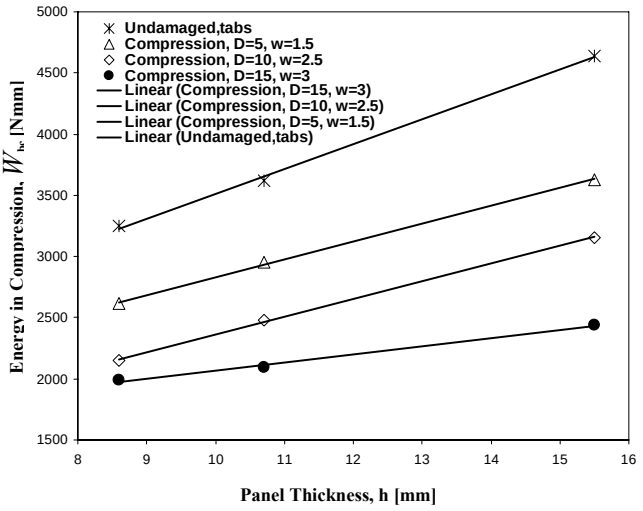

Fig.8. Energy absorbed in bending (compression condition), W_{bc}

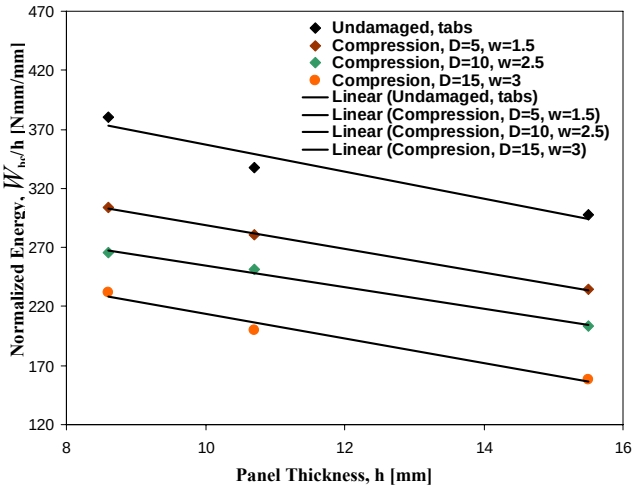

Fig.9. Energy absorbed in bending (compression condition), W_{bc}, normalized by the panel thickness h

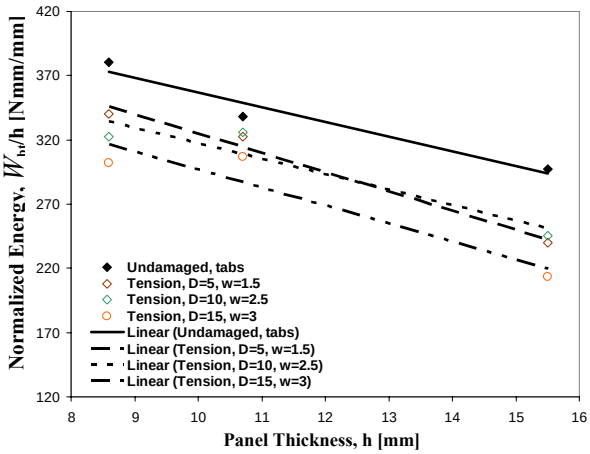

Fig.10. Energy absorbed in bending (tension condition), W_{bt}, normalized by the panel thickness h

The absorbed energy W_{bt} when the contact damage was placed in a tension condition was also analysed. In this case, particularly for the smaller contact damages, the failure did not always occur at the damaged site. Therefore, the actual absorbed energy was not always measured due to the unpredictable failure modes. However, it was found that there is a similar trend in Fig. 9 and Fig. 10, except for the values of W_{bt}, which are higher than the values of W_{bc}. This difference is explained bearing in mind that the undamaged skin in the damaged zone stiffens the panel when the skin is loaded in tension while in the compression condition the skin has buckled and does not contribute to the panel stiffness. Therefore, for the same contact damage, a larger amount of energy is absorbed by the panel if the damage is located in the tensile zone of the beam, than if it is placed in the compressive zone.

3.3 Remnant Strength

At first, the strength of the undamaged samples was measured using the fixture shown in Fig. 2(a). The results reveal that load lines or continuous indentations were formed beneath the loading rollers (Fig. 11), due to a stress concentration caused by the distribution of the load over a small area. To reduce the incidence of roller-induced contact damage, and to obtain more reliable results, tabs were placed under the loading rollers (Fig. 2(b)). Consequently, the failure mode of the samples changed and the panels usually failed in the middle of the beam where the skin buckled in compression and detached from the foam (Fig. 12). From the observation, the foam core at that point sheared.

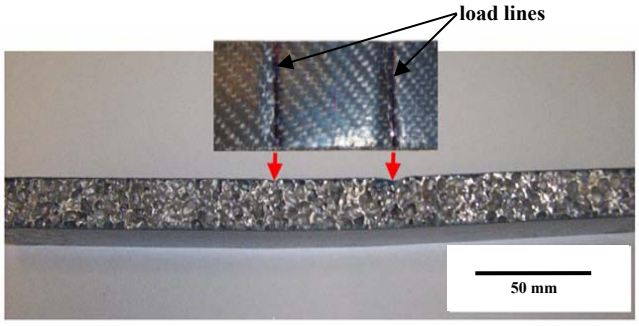

Fig.11. Load lines under the loading rollers

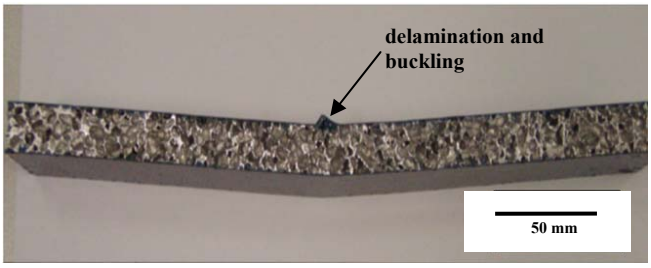

Fig.12. Delamination and buckling of the skin

The bending strength of all the undamaged samples with and without tabs was calculated using Eq. 1, (Fig. 13). It appears that if no tabs are applied, the bending strength is lower than if tabs are used. For samples with tabs, the average bending strength in the skin is ≈ 370 MPa:

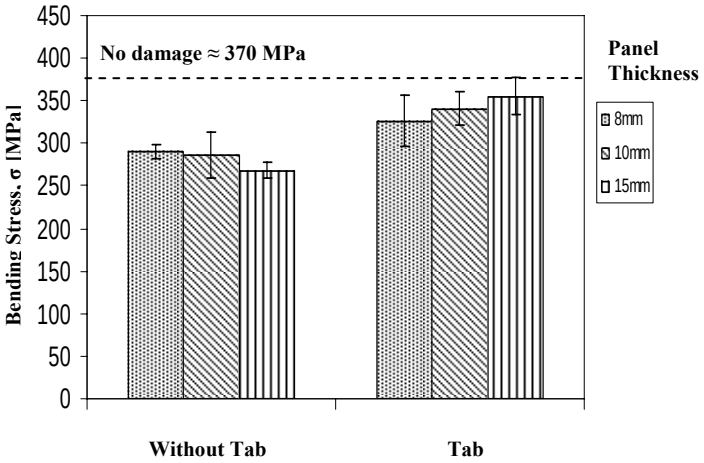

Fig.13. Bending strength of undamaged samples with and without tabs

Next, the compressive and the tensile strength (normalised by h) was calculated for all the damaged samples. This calculation was done using Eqn. 1 and Eqn. 3. When the bending strength was calculated from the initial panel thickness, the undamaged samples exhibited a higher strength at failure than the damaged samples. Thus, the bending strength decreases with the damaged volume increasing, which is illustrated in Fig. 14 in both tension and compression condition, for 8 mm thick panels. This figure is representative for all the samples and core thicknesses; it also reveals that for the same damage volume, the tensile strength is much higher than the compressive strength. However, for 8 mm thick panels, the tensile bending strength in the damaged samples for indentation depths of 2.5 mm and 3.0 mm, were slightly higher than for the undamaged samples. A possible explanation is that the non-uniformity of the foam core is more influential in thinner panels, which have a smaller number of cells across the sample, and therefore, the results for them are more scattered.

Furthermore, it is predicted that the bending stress at the damaged site is higher than the bending stress calculated for the initial thickness of the sample. This is due to the lower flexural stiffness at the indentation mark which leads to stress concentration there.

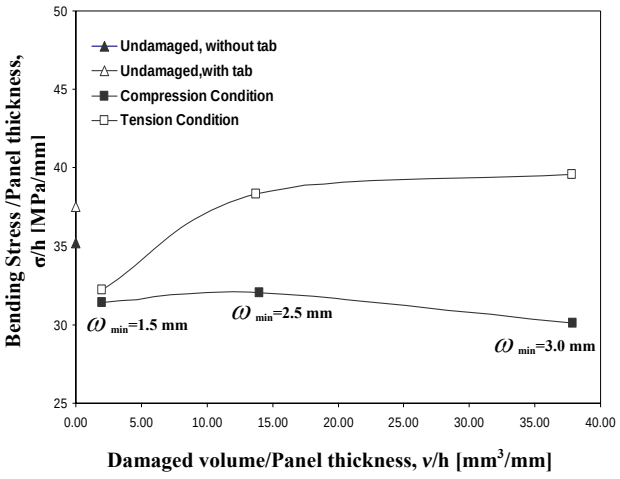

Fig.14. Compressive and tensile strength of 8 mm panel thickness

3.4 Failure Modes

Several failure modes were observed in the four-point bending tests, depending on whether the samples were undamaged or damaged. As previously mentioned, the undamaged samples failed in the middle on the compressive side where the skin buckled and delaminated. For the damaged samples, the failure modes depended on whether the indented region was located on the compressed or on the tensile side of the samples. Under compressive loading, when the samples were indented with smaller spherical indenters and the damaged zone was smaller, the skin broke near the tabs (Fig. 15 (a)) and the foam under it sheared. This could be explained with the stress concentration sites located near the loading tabs. When the samples were indented with larger spherical indenters (10 and 15 mm), however, the skin failed in the damaged zone (Fig. 15 (b)), where the bending stress was high due to the small sample thickness there and the decreased flexural stiffness.

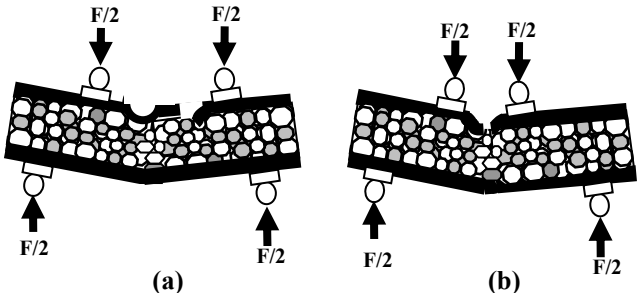

Fig.15. Failure modes if the damaged zone is under a compressive loading condition: (a) the skin breaks near the tabs; (b) the skin fails in the indented area.

Under tensile loading, the thinner samples with smaller damaged zone failed on the undamaged compressive surface. This type of failure was less pronounced than the failure under a compressive loading (Fig.16). For larger damaged zones and thicker samples (Fig. 17) the failure occurs in the damaged zone, in contrast to the failure of thinner samples (Fig. 18). Thus, higher resistance to bending is offered by thicker panels, and larger loads are required to bend and subsequently fail the samples.

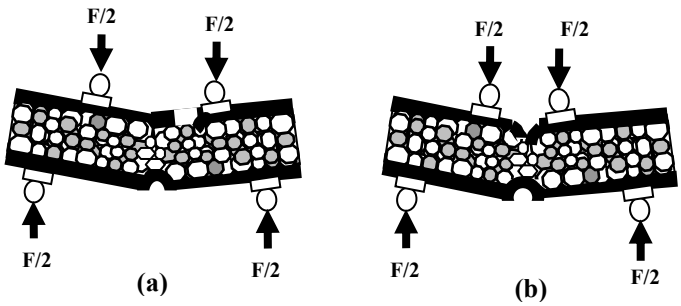

Fig.16. Failure modes if the damaged zone is under a tensile loading condition: (a) the skin breaks near the tabs; (b) the skin fails in the middle of the undamaged surface.

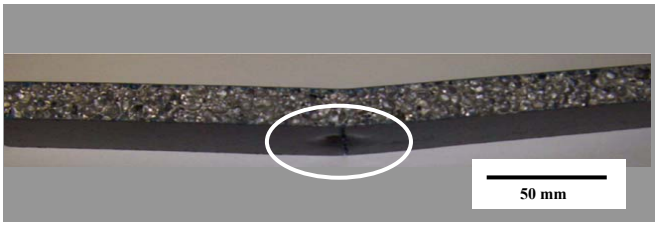

Fig.17. Failure in the damaged zone for thicker samples and larger damaged zones if the damaged zone is in a tensile loading condition.

Fig.18. Thinner samples with no failure; large damaged zone in a tensile loading condition

4 Conclusions

The present paper investigates the residual strength of aluminium closed-cell core sandwich panels stiffened by carbon fibre skin, when locally damaged, and subsequently loaded in bending. It has been found that the contact damage is dependent on the indenter diameter but independent on the sample thickness. The panels' strength is influenced by the extent of the contact damage. The undamaged samples possess higher compressive strength than the damaged samples, whose remnant strength was greatly reduced. The size of the damaged zone affects the strength reduction in bending as the greater the initial damage, the lower the residual strength. The tensile remnant strength was dependent on the sample thickness, although the failure occurred on the undamaged panel surface. The tensile strength decreases as the sample thickness and the damaged size increase. In addition, the failure modes are largely dependent on the loading conditions, compressive or tensile.

Acknowledgement

MI would like to thank the Ministry of Higher Education, Malaysia, and Universiti Tun Hussein Onn Malaysia (UTHM), for their financial support.

References

[1] Vaidya U. K. et *al*. "Impact and post-impact vibration response of protective metal foam composite sandwich plates". *Materials Science and Engineering A,* 428, pp 59-66, 2006.

[2] Villanueva G.R. and Cantwell W.J. "The high velocity impact response of composite and FML-reinforced sandwich structures". *Composites Science and Technology,* 64, pp 35-54, 2004.

[3] Hollaway L "*Polymer composites for civil and structural engineering"*. 1st edition, Blackie Academic & Professional, 1993.

[4] Chen C., Harte A-M. and Fleck N.A. "The plastic collapse of sandwich beams with a metallic foam core". *International Journal of Mechanical Sciences",*43, pp 1483-1506, 2001.

[5] Kesler O. and Gibson L.J. " Size effects in metallic foam core sandwich beams". *Materials Science and Engineering*, A326, pp 228-234, 2002.

[6] Dear J. P., Lee H. and Brown S.A. "Impact damage processes in composite sheet and honeycomb materials". *International Journal of Impact Engineering*, 32, pp 130-154, 2005.

[7] Tagarielli V. L., Fleck N.A. and Deshpande V.S. "Collapse of clamped and simply supported composite sandwich beams in three-point bending". *Composite: Part B*, 35, pp 523-534, 2004.

[8] Crupi V. and Montanini R. "Aluminium foam sandwiches collapse modes under static and dynamic three-point bending". *International Journal of Impact Engineering*, 34, pp 509-521, 2007.

[9] Steeves C.A and Fleck N.A. "Collapse mechanisms of sandwich beams with composite faces and a foam core, loaded in three-point bending. Part I: analytical models and minimum weight design". *International Journal of Mechanical Sciences*, 46, pp 561-583, 2004.